POLITECNICO DI TORINO
Repository ISTITUZIONALE

Impact of the Overall Electrical Filter Shaping in Next-Generation 25 and 50 Gb/s PONs

(Article begins on next page)

04 August 2020

Impact of the Overall Electrical Filter Shaping in Next-Generation 25 and 50 Gb/s PONs

Pablo Torres-Ferrera, Valter Ferrero, Maurizio Valvo, and Roberto Gaudino

Abstract—Next-generation high-speed passive optical networks (HS-PONs) supporting 25, 50, and 100 Gb/s are in the early stages of their standardization process. One key aspect under discussion is the choice of the best modulation format for the transceivers. Performance comparisons among several modulation formats against different physical constraints have been presented in literature and are still being examined. In our present contribution, we performed an exhaustive analysis on the impact of the electrical frequency response of transceivers on the performance of two-level pulse amplitude modulation (PAM-2), 4-level PAM (PAM-4), electrical duobinary, and optical duobinary modulation formats with adaptive equalizers on the receiver side. We show, by means of numerical simulations, that the specification of the typically used −3 dB bandwidth is insufficient, since out-of-band electrical frequency response specifications (such as the −20 dB bandwidth) have a huge impact on the performance of the analyzed modulation formats. We believe that the normalized performance graphs given at the end of the paper in terms of −3 dB and −20 dB bandwidths can thus be useful for the design of next-generation HS-PON transceivers.

Index Terms—Adaptive equalization; APD; Duobinary; Filtering; PAM; PON.

I. INTRODUCTION

Standardization efforts to define the physical layer characteristics of next-generation high-speed passive optical networks (HS-PONs) are currently being carried out in the International Telecommunication Union (ITU), Full Service Access Network (FSAN) Group, and the Institute of Electrical and Electronics Engineers (IEEE) standardization bodies [1–5]. Several research analyses are currently ongoing to choose the best modulation format for HS-PON transceivers for different bit rates under consideration (such as 25, 40, and 50 Gb/s) [6–17]. Due to a low cost constraint, particularly for the optical network unit (ONU) (i.e., user) side, several groups are considering if the transmitter and receiver optoelectronics developed for lower bit rates can be re-used for the new

higher capacity transceivers when associated to more bandwidth efficient modulation formats and/or adaptive equalization (AEQ). In particular, it would be interesting to re-use the optoelectronics developed for a 10 Gb/s PON for the 25 Gb/s target (and even for the 40 or 50 Gb/s ones), and similarly re-use the 25 Gb/s technology developed for the intra-datacenter short-range transceivers, also for 40–50 Gb/s PONs.

The motivation of this work is thus to analyze the feasibility of these goals, focusing on the fact that these transceivers would be severely electrically band-limited when used for the new target bit rates envisioned for HS-PONs (25 and 50 Gb/s). While previous papers in this area usually only focus on the −3 dB bandwidth [18,19], or experimentally on a single given transceiver, we believe our approach is unique because this paper demonstrates, through extensive analyses, the strong impact of the overall frequency transfer function on system performance. We analyzed traditional intensity-modulation transmitters and direct-detection (DD) receivers followed by a digital signal processing (DSP)-based adaptive equalizer. We show that the *out-of-band* transceiver electrical frequency response is important for the modulation formats under consideration that are PAM-2 (i.e., binary on-off keying), PAM-4, electrical duobinary (EDB) [6,11], and optical duobinary (ODB) [8]. Specifically, we provide normalized graphs showing the joint impact of the −3 dB and −20 dB parameters of the frequency response on the system performance. We believe that these graphs offer a useful contribution to the current discussion in the aforementioned HS-PON standardization bodies and to the transceiver vendors that, depending on the details of their optoelectronic technology, can better select how to optimize their component design.

Thanks to our simulative approach, we were able to span a very large set of parameters (−3 dB bandwidth, −20 dB bandwidth, accumulated dispersion, etc.) and then obtain power penalty curves at a specific bit error rate (BER) value for the four different modulation formats. Moreover, we superimposed on our simulative results the expected bandwidths of several existing transmitters and receivers, thus giving a very broad review of the existing literature in this field.

Summarizing our previous considerations, we believe that the main contribution of this paper is in offering design rules for the transceivers' full electrical frequency

response for different modulation formats. Consequently, our analysis points out the different resiliencies of each modulation format to variations in the available bandwidth and provides information that again can be interesting for component designers. We also report an extensive review of the transfer function of many transmit and receive options (TXs and RXs) presented in the literature, and we give their positioning in our performance estimation graphs.

To this end, the paper is organized in six sections. In Section II, we present the details of the considered transceiver and link architecture and of our simulation environments. In Section III, we discuss different frequency response characteristics, and apply it in Section IV, evaluating the resulting power budget penalty versus filter shape parameters. In Section V, we also introduce the impact of the typical chromatic dispersion accumulated in a PON for different choices of the wavelength band. Finally, we draw a conclusion in Section VI.

II. SIMULATION SETUP

The transceiver and link architecture that we considered in our simulation setup is shown in Fig. 1, where the variable optical attenuator (VOA) is used to span different values of link loss, including the impact of the $1 \times N$ PON splitting ratio. For space limitation, we will not consider the penalty arising from burst mode transmission. Apart from this (important [20]) consideration, our analysis can be applied to both the downstream and upstream directions of a PON link.

At the transmitter side, a binary signal at bit rate R_b (equal to either 25 or 50 Gb/s) is generated by means of a pseudorandom bit sequence (PRBS) $2^{17} - 1$ bits long. The bit stream feeds the electrical TX that creates the appropriate driving signal to generate PAM-2, PAM-4, EDB, or ODB signals in the optical domain. We considered the use of external modulation in this paper or more in general optical transmitters characterized by negligible chirp. The generated electrical signal indicated as $x(t)$ in Fig. 1 is obtained in different ways depending on the modulation format:

(i) In PAM-2 and PAM-4 cases, the binary signal is mapped into a 2-level or 4-level symbol stream, respectively. Gray coding is used in PAM-4.

(ii) In both EDB and ODB cases, the binary signal is digitally pre-coded by applying a standard XOR-based scheme [11]. The resulting 2-level pre-coded signal will eventually turn into a 3-level DB signal thanks to the intrinsic low-pass filtering response of the transceiver. We avoid the use of additional add-and-delay encoding or low-pass electrical filter circuits.

Time-domain simulations are performed using internally developed code fully written in a well-known commercial numerical software. Eight samples per bit (spb) were set. The signal $x(t)$ is normalized to $0 \leq x(t) \leq 1$. We then assume that the DSP can compensate the Mach-Zehnder modulator (MZM) $\cos^2(\cdot)$ instantaneous nonlinear response by applying the pre-distortion,

$$x_D(t) = \frac{A}{\pi} \arccos(1 - 2x(t)) - V_b, \qquad (1)$$

where A is an amplitude factor and V_b is the bias-voltage of the MZM. The pre-distorted signal $x_D(t)$ is then filtered using an electrical low-pass filter (LPF) that emulates the electrical frequency response of the TX. The shape of this filter (and the following one at the RX) is one of the main goals of our investigation. Details on the assumed filter shapes will be given in the Section III. The resulting electrical signal after filtering, $x_F(t)$, drives an optical modulator, optically fed by a continuous wave (CW) electrical field, $E_{CW}(t)$, generated by the TX laser. The electrical LPF, the optical modulator, and the laser compose the externally modulated laser (EML) block. The optical signal at the output of the EML is modeled using a classical (chirpless) MZM equation,

$$E_{EML}(t) = E_{CW}(t) \cos \frac{\pi x_F(t)}{V_\pi}, \qquad (2)$$

where V_π is the π-voltage of the modulator. By setting both parameters, A and V_b, of Eq. (1) equal to $V_\pi/2$ for PAM-2, PAM-4, and EDB, or equal to V_π for ODB, the MZM is operated in quadrature or null, respectively. The modulated optical signal is then propagated through a conventional single-mode fiber (SMF). Only chromatic dispersion is considered in the fiber model since the nonlinear effects are assumed to be negligible for the relatively short reach (≤ 20 km) applications and power levels under study. The received optical signal is detected by means of an avalanche photodetector (APD) at the receiver (RX) side followed by a transimpedance amplifier (TIA). The APD + TIA configuration currently seems to be the most likely to be applied for a 40-gigabit-capable PON (NG-PON2) and a 10-gigabit-capable symmetric PON (XGS-PON), which is why we decided to focus on it. The photocurrent that outputs the APD + TIA is evaluated by
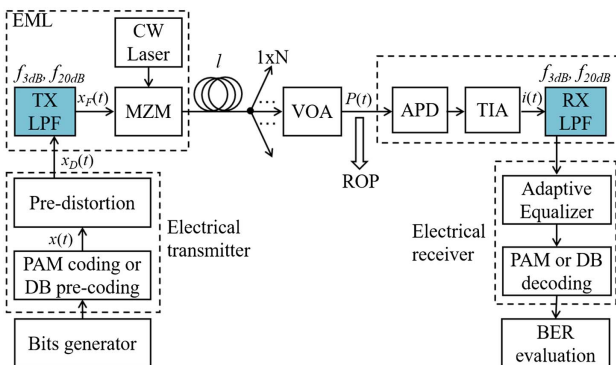
$$i(t) = GRP(t) + n_S(t) + n_T(t), \qquad (3)$$

F1:1   Fig. 1.   Simulation setup.

where R is the APD responsivity (assumed to be $R = 0.8$ A/W), G is the APD gain factor [assumed to be $G = 25$ (14 dB)] [21,22], and $P(t)$ is the optical signal instantaneous power that feeds the APD. The signals $n_S(t)$ and $n_T(t)$ emulate the shot noise and thermal noise, respectively. They are modeled as Gaussian random processes with zero-mean and variances given by [23]

$$\sigma_S^2(t) = qG^2 F R P(t) \Delta f_s, \qquad (4)$$

$$\sigma_T^2 = N_0 \Delta f_s, \qquad (5)$$

respectively, where F is the APD excess noise factor (we assumed $F = G^{0.75} = 10.5$ dB), q is the electron charge, N_0 is the input-referred electrical current thermal noise power spectral density ($N_0 = 1.024 \times 10^{-21} A^2/$Hz), and Δf_s is the bandwidth of the simulation ($\Delta f_s = $ spb $\cdot R_b$). The overall thermal noise of APD and TIA contributions are included in the $n_T(t)$ noise term. The numerical values assumed here are just indicative values for today's typical 10G PON receivers. Since we present our results in terms of the relative power penalty among different modulation formats (see Sections IV and V), their actual values, however, will have relatively little impact on the penalty graphs.

After the APD + TIA, an electrical LPF emulates the RX frequency response. The characteristics of this RX LPF are the same as the TX LPF, and they are described in the next section. We know that this is not the more general case since the TX and RX filter shapes are independent. We introduce this assumption to limit the number of free parameters to be spanned. In the next section, an extended discussion regarding this consideration is presented.

Since we want to focus on severely band-limited transceivers, we assume that the received electrical signal is equalized by an adaptive feed-forward equalizer (FFE) using least-mean square (LMS) as an adaptation algorithm [19,24] with two samples per symbol and 20 taps. This number of taps was selected to guarantee the right operation of the system in very dispersive and band-limited scenarios. In some cases, however, the system can operate with fewer taps without an additional penalty. The equalizer is trained with a proper pilot sequence, which for PAM-2, PAM-4, and ODB is simply the original transmitted symbol sequence. For EDB, we use a 3-level DB symbol stream obtained after encoding the input pre-coded signal by means of an add-and-delay block. The equalized signal is then decoded according to the employed modulation format. Finally, the bit error rate (BER) is evaluated using direct error counting over 1.3×10^5 bits (after the training sequence), a situation that is very CPU-time demanding, but allows very precise estimation of the BER around the 10^{-3} target value.

The main figure of merit employed in this work to evaluate the performance of the system is the sensitivity (S), defined as the received optical power (ROP) in dBm to reach a BER target of 10^{-3} (i.e, the pre-FEC value selected, for instance, for NG-PON2 in ITU-T G.989.2 for 10 Gb/s).

III. FILTERING CONSIDERATIONS

We emulate narrowband transceivers using two electrical LPFs, one at the TX side and one at the RX side. One key parameter of a transceiver frequency response is obviously its –3 dB electrical bandwidth ($f_{3\,dB}$). Most of the experimental and commercial device characterizations provide information about this parameter. However, as the main target of our work, we focus on the fact that not only the $f_{3\,dB}$ parameter is fundamental, but the out-of-band (i. e., $f > f_{3\,dB}$) frequency response of the devices also has a strong impact on the overall system performance. We show, for instance, that for the same $f_{3\,dB}$ value, very different performance can be achieved depending on the actual value of, say, the –20 dB bandwidth. Moreover, we will show that the sensitivity versus this last parameter is very different, depending on the modulation format used. To the best of our knowledge, this is a novel analysis for the HS-PON scenario, since the out-of-band transceiver electrical frequency characterization is barely ever considered in detail in the available literature. To investigate the relevance of this out-of-band filter shaping, we introduce the –20 dB bandwidth parameter ($f_{20\,dB}$) in our present analysis. The joint impact of the $f_{3\,dB}$ and the $f_{20\,dB}$ parameters is then tested, providing an extra degree of information regarding the impact of the filtering shape on the performance. We present most of our results using the parameters $B_{3\,dB}$ and $B_{20\,dB}$, which are a representation of $f_{3\,dB}$ and $f_{20\,dB}$, respectively, normalized to the bit rate, expressed in percentages, and thus defined as

$$B_{3\,dB}[\%] = \frac{f_{3\,dB}}{R_b} \times 100 \quad \text{and} \quad B_{20\,dB}[\%] = \frac{f_{20\,dB}}{R_b} \times 100. \quad (6)$$

The degrees of freedom in electrical filter shapes are obviously infinite, so we had to make a somewhat arbitrary decision and select a few canonical transfer functions used in the literature [25]. We opted for the Butterworth (BF) and super-Gaussian filter (GF) profiles. Because the former is straightforward, it was selected to exactly set the desired $f_{3\,dB}$ parameter and to characterize it in terms of the number of poles [25]. Moreover, the BF frequency response is as flat as possible in the passband [25], thus reducing, as compared to other filter types, the in-band shape variations (for a fixed passband bandwidth) when changing the out-of-band steepness. This feature is useful if researchers want to analyze the impact of the out-of-band shape variations as independently as possible on the in-band shape changes (as in the present contribution). However, in BF and for a fixed $f_{3\,dB}$, the value of the $f_{20\,dB}$ parameter is subject to the choice of the number of poles of the filter (that is, an integer number) and, consequently, $f_{20\,dB}$ can be only changed over given (and quite coarse) discrete values. Therefore, for BF, it is not possible to set any arbitrary combination of the $f_{3\,dB}$ and $f_{20\,dB}$ parameters. The use of GFs overcomes this limitation by allowing an independent variation of $f_{3\,dB}$ and $f_{20\,dB}$. The frequency profile of a GF is defined here as [26]
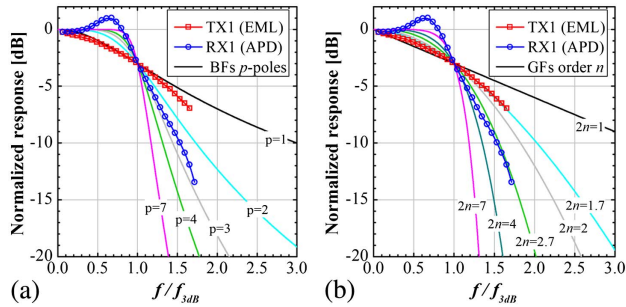
Fig. 2. (a) Butterworth (BF) and (b) Super-Gaussian filter (GF) profiles, for different numbers of poles and order, respectively. The normalized experimental response of the TX (EML) and the RX (APD) found in literature [17] are also shown.

$$H(f) = \exp\left(-\frac{1}{2}\left(\frac{f}{f_0}\right)^{2n}\right), \qquad (7)$$

284 where n is the order of the GF filter (which now does not
285 necessarily need to be an integer) and f_0 is a free param-
286 eter. The two free and real values, n and f_0, can be set to
287 obtain a frequency response having any possible combina-
288 tion of $f_{3\,dB}$ and $f_{20\,dB}$ (as long as $f_{20\,dB} \geq f_{3\,dB}$). In Figs. 2(a)
289 and 2(b), the filter shape profiles of the BF and GF models,
290 respectively, are presented for different numbers of poles
291 and order, using on the x-axis as the frequency normalized
292 to $f_{3\,dB}$. The frequency responses of a realistic TX-RX pair
293 experimentally reported in [17] are also displayed in the
294 figure. From Fig. 2 it can be seen that, after a proper fitting
295 of its two degrees of freedom, the GF model allows a good
296 emulation of the out-of-band frequency response of the
297 realistic TX and RX. The fitting using the BF model is less
298 precise, due to the aforementioned discretization on the
299 number of poles. This result also shows that a realistic
300 transceiver cannot be easily modeled using zeros and poles
301 rationale transfer functions if one must emulate accurately
302 the frequency response also above the 3 dB band. Having
303 said this, most of the results in Sections IV and V will be
304 presented for both GF and BF models to have a full view of
305 the filter shaping problem.

306 The most significant simplifying assumption made in
307 this work is that the TX and RX LPFs are identical (i.e.,
308 they have the same filter shape). Although, this approach
309 may not appear very realistic, a systematic analysis testing
310 different combinations of $f_{3\,dB}$ and $f_{20\,dB}$ values in both the
311 TX and RX filters would require studying a huge number of
312 cases and several degrees of freedom, which is very imprac-
313 tical. We found that the equivalent filter formed after cas-
314 cading any pair of TX and RX identical LPFs can approach
315 well the overall equivalent frequency response formed by
316 any particular combination of real TX and RX devices with
317 different filter shaping (i.e., TX and RX with different $f_{3\,dB}$
318 and $f_{20\,dB}$ values). As a practical example, the same TX-RX
319 pair taken from [17] and already represented in Fig. 2 (TX1
320 EML $f_{3\,dB} = 8.9$ GHz, RX1 APD $f_{3\,dB} = 7.5$ GHz) is used
321 again in Fig. 3 to obtain the concatenated TX + RX transfer
322 function, shown by a solid black curve. On the same figure,
323 the response of the cascade of two identical GFs (or BFs) is
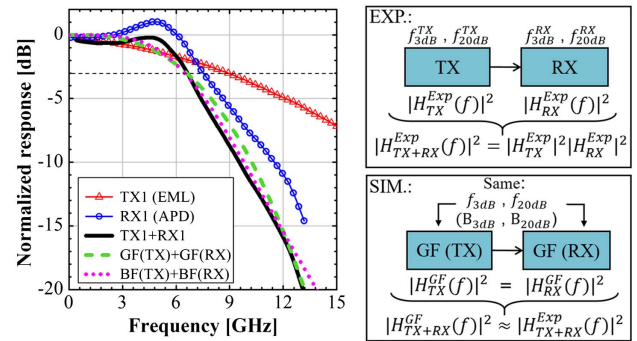324 shown in dashed green (or dotted pink, for a pair of

Fig. 3. Left side: TX (EML) and RX (APD) frequency characteri-   F3:1
zation reported in [17]. In solid black, the TX+RX equivalent re-   F3:2
sponse. In dashed (dotted), the equivalent frequency response of   F3:3
a pair of identical GFs (BFs), with the same $B_{3\,dB}$ and $B_{20\,dB}$.   F3:4
Right side: Diagram of our employed best-fitting procedure   F3:5
(EXP, Experimental data, and SIM, Simulation approach).   F3:6

325 identical BFs) curve. In the case of GFs, a good matching
326 with the solid black curve was obtained with two identical
327 GFs, each with $f_{3\,dB}$ equal to 8.5 GHz and $f_{20\,dB}$ equal to
328 17 GHz. The equivalent pair of identical BFs are 2-pole
329 filters, each with $f_{3\,dB}$ equal to 8.1 GHz.

330 We followed this fitting procedure (shown in Fig. 3) for a
331 large set of experimental devices reported in the literature.
332 In particular, we evaluated the $f_{3\,dB}$ and $f_{20\,dB}$ values
333 (and corresponding $B_{3\,dB}$ and $B_{20\,dB}$) of the GFs whose cas-
334 caded responses best matched the cascaded response of ex-
335 perimental or commercial TX + RX devices (see Fig. 3,
336 right-hand diagram), and we summarized the results in
337 Table I. Please note that all of these TX and RX devices
338 were developed for standard NRZ 10 Gb/s transmission,
339 which we will label in the rest of the paper as *10G*

TABLE I
NORMALIZED (FOR 25 OR 50 Gb/s TRANSMISSION) −3 dB AND
−20 dB BANDWIDTH ($B_{3\,dB}$ AND $B_{20\,dB}$) FOR EACH OF THE
IDENTICAL GFs AT TX AND RX WHOSE CASCADE RESPONSE BEST
FITS THE EQUIVALENT RESPONSE OF THE TX + RX 10G
COMPONENTS REPORTED IN THE REFERENCES

C.	TX (Exp.) Ref.	$f_{3\,dB}^{TX}$	RX (Exp.) Ref.	$f_{3\,dB}^{RX}$	GF, $R_b = 25$ $B_{3\,dB}$	$B_{20\,dB}$	GF, $R_b = 50$ $B_{3\,dB}$	$B_{20\,dB}$	
									T1:1
									T1:2
1	[17]	8.9	[17]	7.5	34	68	17	34	T1:3
2	[17]	8.9	[28]	8.8	32.8	112	16.4	56	T1:4
3	[17]	8.9	[29]	8.1	32	136	16	68	T1:5
4	[17]	8.9	[22]	6.8	29.6	96	14.8	48	T1:6
5	[27]	7.7	[17]	7.5	32	56	16	28	T1:7
6	[27]	7.7	[28]	8.8	27.6	80	13.8	40	T1:8
7	[27]	7.7	[29]	8.1	28	96	14	48	T1:9
8	[27]	7.7	[22]	6.8	26.8	72	13.4	36	T1:10
9	[a]	9.9	[17]	7.5	34	70	17	35	T1:11
10	[a]	9.9	[28]	8.8	35.2	100	17.6	50	T1:12
11	[a]	9.9	[29]	8.1	34.8	128	17.4	64	T1:13
12	[a]	9.9	[22]	7.5	31.6	92	15.8	46	T1:14
13	[30][b]: $f_{3\,dB}^{Sys} = 6.3$ GHz				33.2	70	16.6	35	T1:15

C.: Case. $f_{3\,dB}^{TX}$ and $f_{3\,dB}^{RX}$ in GHz. $B_{3\,dB}$ and $B_{20\,dB}$ in %. R_b in Gb/s.
[a]NG-PON2 TX characterization provided by Telecom Italia.
[b]In this particular case, $f_{3\,dB}^{Sys}$ indicates: $f_{3\,dB}$ of the overall system.

TABLE II

NORMALIZED (FOR 50 Gb/s TRANSMISSION) −3 dB AND −20 dB
BANDWIDTH ($B_{3\,dB}$ AND $B_{20\,dB}$) OF EACH OF THE IDENTICAL GFs
AT TX AND RX WHOSE CASCADE RESPONSE BEST FITS THE
EQUIVALENT RESPONSE OF THE TX + RX 25G COMPONENTS
REPORTED IN THE REFERENCES

		TX (Exp.)	RX (Exp.)		GF, $R_b = 50$ Gb/s	
T2:1						
T2:2	C.	Ref.	[GHz]	Ref.	$f_{3\,dB}^{RX}$ [GHz]	$B_{3\,dB}$%	$B_{20\,dB}$%

C.	Ref.	[GHz]	Ref.	$f_{3\,dB}^{RX}$ [GHz]	$B_{3\,dB}$%	$B_{20\,dB}$%
T2:3 **1**	[31]	18.9	[33]	15.8	34	60
T2:4 **2**	[31]	18.9	[34]	24.5	40	132
T2:5 **3**	[31]	18.9	[35]	32	45	140
T2:6 **4**	[31]	18.9	[36]	19.9	40	88
T2:7 **5**	[32]	28.2	[33]	15.8	32	58
T2:8 **6**	[32]	28.2	[34]	24.5	50	130
T2:9 **7**	[32]	28.2	[35]	32	50	110
T2:10 **8**	[32]	28.2	[36]	19.9	44	88
T2:11 **9**	[27]	23.9	[33]	15.8	30	58
T2:12 **10**	[27]	23.9	[34]	24.5	42	84
T2:13 **11**	[27]	23.9	[35]	32	44	90
T2:14 **12**	[27]	23.9	[36]	19.9	38	78

340 *technology*. In Table II, the same information is reported for
341 another set of experimental devices reported in literature
342 for the 25 Gb/s transmission, called in this paper 25G tech-
343 nology. The information provided in Tables I and II is very
344 helpful to contextualize our results in the framework of
345 state-of-the-art technology.

346   From Table I, we can observe that the same couple of TX-
347 RX devices has associated with a different pair of $B_{3\,dB}$ and
348 $B_{20\,dB}$, depending on the value of R_b. This arises because,
349 although the $f_{3\,dB}$ and $f_{20\,dB}$ parameters of the correspond-
350 ing identical GFs are the same irrespective of R_b, the $B_{3\,dB}$
351 and $B_{20\,dB}$ values are normalized to the bit rate, as
352 indicated in Eq. (6).

353   IV. BACK-TO-BACK RESULTS

354   A back-to-back (BtB) performance comparison among
355 the four modulation formats is presented in this section.
356 For BtB, we mean a simulation that emulates the trans-
357 ceiver bandwidth limitations (thus taking into account only
358 the filtering effects in the TX and RX), the electro-optical
359 and opto-electrical conversions, and the noise at the
360 receiver. The effect of the fiber (i.e., chromatic dispersion)
361 will then be introduced in the next section.

362   We started the BtB analysis by considering 1-pole BFs as
363 the electrical frequency response of each TX and RX device.
364 In the inset of Fig. 4(a), we report the filter profiles of
365 the individual TX, or RX, 1-pole BF (solid) and the cascaded
366 response of them (dotted), for a (single filter) $f_{3\,dB} = 7$ GHz.
367 To enable a fair comparison, the performance is evaluated
368 in terms of the power penalty taking as a reference the sen-
369 sitivity of PAM-2 in its optimal conditions (without any BW
370 limitations and in a BtB scenario). This sensitivity (the
371 ROP to guarantee 10^{-3} BER) is termed S_0, and, for the
372 APD noise levels reported in the previous section, it is
373 equal to $S_0 = -28.1$ dBm for $R_b = 25$ Gb/s, and $S_0 =$
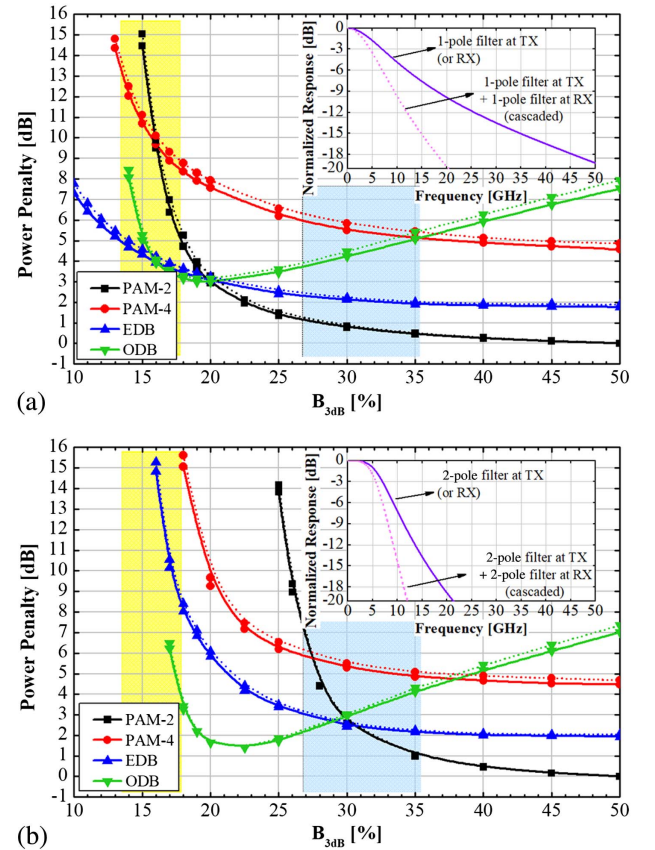374 −25.7 dBm for $R_b = 50$ Gb/s. The computed power penalty

(a)

(b)

Fig. 4. Performance comparison among modulation formats in
terms of the power penalty with respect to S_0, the PAM-2 sensitiv-
ity in the best condition (BtB unlimited bandwidth case, $S_0 =$
−28.1 dBm for 25 Gb/s and $S_0 = -25.7$ dBm for 50 Gb/s), as a
function of the $B_{3\,dB}$ of the filters. (a) 1-pole BF and (b) 2-pole
BF (depicted in the inset). Solid lines for $R_b = 25$ Gb/s, dotted
lines for $R_b = 50$ Gb/s. Colored regions: In blue (yellow): 10G tech-
nology to transmit 25 (50) Gb/s.

of each modulation format as a function of the $B_{3\,dB}$ param-
eter is shown in Fig. 4(a), for both analyzed bit rates:
25 Gb/s (solid) and 50 Gb/s (dotted). Thanks to the em-
ployed definition of the power penalty, there is a very close
match between the results of the two analyzed bit rates, as
demonstrated by the fact that the difference between the
solid (25 Gb/s) and dotted (50 Gb/s) curves is negligible ir-
respective of the modulation format. By using the informa-
tion provided in Table I, we also superimposed on Fig. 4 a
pair of colored regions that qualitatively indicate the range
of $B_{3\,dB}$ values that current 10G technology transceivers
exhibit when transmitting at 25 Gb/s (in blue) and
50 Gb/s (in yellow).

   From Fig. 4 we can observe that in spite of using AEQ,
the impact of limited system bandwidths is not completely
canceled (as expected for an FFE-LMS-based AEQ [24] op-
erating over a noisy signal). However, we have verified that
the penalty due to system bandwidth reduction is much
less pronounced using the AEQ scenario considered in this
paper than for a not-equalized receiver (we cannot show
the relative comparison here due to space limitations).

As discussed in the previous section, a 1-pole filter is very likely too optimistic for most realistic transceivers. To explore the impact of the out-of-band filter shaping on the analyzed modulation formats performance, the procedure to obtain the results presented in Fig. 4(a) is performed again using 2-pole BFs, but keeping the other assumptions the same. The corresponding results obtained under this new situation are presented in Fig. 4(b). One of the key points of our paper can be seen here: The out-of-band steepness of the transceivers' frequency response significantly affects the system performance even for the same −3 dB bandwidth, and changes the performance ranking of the different modulation formats. For instance, let us consider the transmission of 25 Gb/s using 10G technology-based transceivers (case referred here as 25G/10G, shown in the blue-colored area of Fig. 4). In this situation, if the transceiver response is modeled using a 1-pole BF approach, PAM-2 outperforms the rest of the modulation formats in the complete 25G/10G (blue) region. However, if the filter's response model changes from one- to two-pole BF [Fig. 4(b)] PAM-2 starts to become critical, and it is, for instance, surpassed by EDB in part of the 25G/10G region of the graph. As another example, let us now consider the transmission of 50 Gb/s using 10G technology (case referred to here as 50G/10G, shown in the yellow colored area of Fig. 4). From Fig. 4(a), we can observe that EDB, ODB, and even PAM-4 (with a strong penalty) could be feasible alternatives for the 50G/10G transmission if a 1-pole filter case is considered (while PAM-2 is clearly out of the question). If we again change the filter response to a 2-pole profile, we can see from Fig. 4(b) that even EDB, ODB, or PAM-4 would operate in a region with exceedingly high penalty.

These first two examples show the performance dependency of the modulation formats versus the transceivers' frequency response, not only in terms of the −3 dB bandwidth (as commonly done in much of the analysis in the current literature), but also as a function of the out-of-band (i.e., above the −3 dB point) filter steepness.

We thus prosecute our analysis by also considering a parameter that would characterize the out-of-band response. As mentioned in Section III, we selected for this goal the frequency at a −20 dB attenuation (i.e., the $f_{20\,dB}$ parameter and its normalized version, $B_{20\,dB}$). Note that another reference attenuation value could also have been chosen to quantify the degree of tilting of the out-of-band response. The use of the −20 dB attenuation value was selected arbitrarily but, as we will show, it turned out to be a very relevant parameter.

To start the out-of-band filter impact analysis, we fixed the $B_{3\,dB}$ parameter to 28%, which is a representative state-of-the art case for the 25G/10G transmission as shown in Table I, and varied the number of poles of the BFs. As shown in Fig. 2(a), for a BF with a given $f_{3\,dB}$, increasing the number of poles corresponds to an increase in the out-of-band filter steepness, and a decrease in its −20 dB bandwidth. The performance of the four modulation formats in terms of the relative power penalty as a function of the BF number of poles (or the corresponding $B_{20\,dB}$ parameter) is shown in Fig. 5 (markers only), for 25 Gb/s transmission.
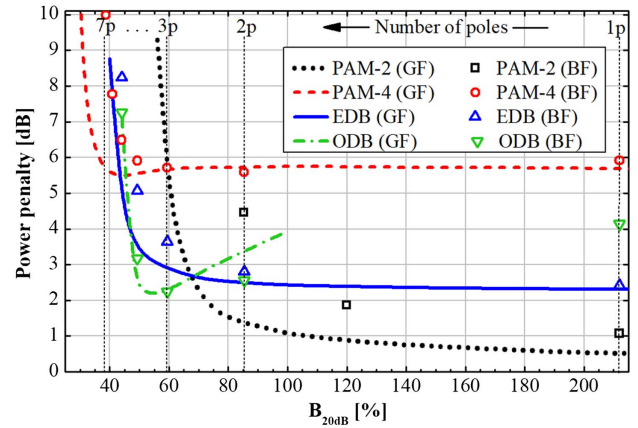

Fig. 5.   Performance comparison in terms of $B_{20\,dB}$ using BF (only marker curves) and GF (only line curves). A 25 Gb/s transmission is considered. The $B_{3\,dB}$ is fixed to 28% ($f_{3\,dB} = 7$ GHz for $R_b = 25$ Gb/s). The power penalty is relative to PAM-2 $S_0 = −28.1$ dBm for $R_b = 25$ Gb/s.

Since the number of poles is an integer parameter, only certain discrete $B_{20\,dB}$ values can be evaluated. To overcome this too coarse discretization of $B_{20\,dB}$, the use of the GF model to emulate the transceiver frequency response is introduced. Under this GF approach, continuous curves of a relative power penalty versus $B_{20\,dB}$ can now be obtained, and are depicted in Fig. 5 (curves without markers). Apart from the differences that occur using the BF or GF model, Fig. 5 shows with evidence the great relevance of the exact value of the out-of-band filter shape and, again, the fact that the performance ranking among modulation formats is also greatly affected by this parameter. For instance, although PAM-2 is the best modulation format in the $B_{20\,dB} > 120\%$ region, for $B_{20\,dB} \leq 70\%$ PAM-2 starts to become exceedingly critical in terms of the penalty. The EDB solution has, on the contrary, a good resilience for low $B_{20\,dB}$ values, showing just small penalties down to the $B_{20\,dB} = 50\%$ region. PAM-4 also exhibits a good tolerance, even for $B_{20\,dB} = 40\%$. ODB has a very peculiar behavior, showing both in Fig. 4 (versus $B_{3\,dB}$) and Fig. 5 (versus $B_{20\,dB}$) that it may be considered the best modulation format for very low bandwidths, but only if the $B_{3\,dB}$ and $B_{20\,dB}$ are optimized to their proper values. However, for $B_{20\,dB} > 60\%$ values, the ODB sensitivity starts to get worse. The increased penalty shown with the GF approach is attributed to the reduced in-band power that this filter collects with respect to BFs for higher values of $B_{20\,dB}$ (see Fig. 2). In the case of PAM-2, a close match between the BF and GF filter shape is only found when the filter steepness is very low (around the 1-pole BF case). Please note that for PAM-2, a point between the 1- and 2-pole cases was plotted. This point was measured by setting a 1-pole filter at the TX and a 2-pole filter at the RX (which corresponds to a 3-pole filter when the TX and RX filters are cascaded, emulating symmetric 1.5-poles at the TX and RX situation). This is the only exceptional point that was evaluated using different characteristics at TX and RX filters in this contribution. However, following the same approach, the performance of the system using a 1-pole filter at the TX and a 3-pole filter

at the RX was also tested for PAM-2 (corresponding to a 4-pole filter when cascading the TX and RX, equivalent of having a 2-pole filter at the TX and one at the RX if a linear system is assumed). The sensitivity measured under this situation was the same as having 2-pole filters at TX and RX, which shows that the system behavior is mostly linear, and the cascaded assumptions described in Section III can be considered accurate.

To summarize, Fig. 5 suggests that when ranking the modulation format tolerance against the variation of the $B_{20\,dB}$ parameter, PAM-4 and EDB show the best degree of resilience, PAM-4 being the most robust format for extremely low $B_{20\,dB}$, but obviously starting from its intrinsic penalty that is present compared to PAM-2 for high bandwidths. ODB has very interesting performance, but only for an optimized filter bandwidth, while EDB shows a very good compromise on a very large range of $B_{20\,dB}$ values.

Compared to the actual data extrapolated from commercial transceivers and reported in the aforementioned Tables I and II, we can see that the $B_{20\,dB}$ parameter can vary from around 60% to even 140%, for different state-of-the-art devices. This fact highlights the need to consider the robustness of a modulation format against both in-band and out-of-band filter shaping variations as a relevant parameter.

The results shown in Fig. 5 were obtained for a fixed value of $B_{3\,dB} = 28\%$. For different $B_{3\,dB}$ values, the conclusions may change. We thus performed an extensive study on the impact of a joint variation of the $B_{3\,dB}$ and $B_{20\,dB}$ parameters. Results are presented in Fig. 6, which shows the power penalty of PAM-2 with respect to its best sensitivity S_0 ($S_0 = -28.1$ dBm for $R_b = 25$ Gb/s, and

$S_0 = -25.6$ dBm for $R_b = 50$ Gb/s) as a function of both $B_{3\,dB}$ and $B_{20\,dB}$ variables. We believe this is one of the key results of our paper, giving transceiver designers an overview of the best system solutions. Using this graph, a component designer can trade off the component parameters that most affect the $B_{3\,dB}$ and $B_{20\,dB}$, and use the best design choices.

In Fig. 6, the contour plots in solid lines correspond to the 25 Gb/s case, while the ones in dotted lines to the 50 Gb/s transmission. A very good agreement between the solid and dotted curves is again found. Tables I and II show the real frequency response characteristics of the transceivers, which are also displayed in Fig. 6, in which any pair of $B_{3\,dB}$ and $B_{20\,dB}$ is considered as the coordinates of a point in the plane (indicating the operation regions of the current devices). Note the huge transceiver filter shaping impact on the performance. For instance, when using 25G transceivers for 50 Gb/s transmission (pink triangles), considering different real devices we can have a negligible penalty (lower than 0.2 dB in some cases), but in other cases the penalty can reach 10 dB. The same information is plotted in Fig. 7 for the other modulation formats, always evaluating the power penalty with respect to the same PAM-2 S_0 sensitivity values of Fig. 6. Since the same good agreement between the 25 and 50 Gb/s results found for PAM-2 was also corroborated for the other modulation formats, only 50 Gb/s curves (representing both bit rate situations) are shown.

By summarizing all the information provided by Figs. 4–7, we can state the following conclusions with respect to the filter shape impact on the performance of the four different modulation formats in the BtB situation. Let us start by considering the options to transmit 25 Gb/s using 10G technology transceivers (25G/10G):

– PAM-4 exhibits the best tolerance against filter shaping variations, in the sense that its penalty curve versus the reduction in filter bandwidth (for both $B_{3\,dB}$ and $B_{20\,dB}$) remains flat down to very low values. However, this format has a bigger penalty compared to EDB or ODB in the 25G/10G region [see the red points of Figs. 7(a)–7(c), and their associated power penalty].

– ODB exhibits large variations as a function of the $B_{3\,dB}$ and $B_{20\,dB}$ parameter. In the search for low transceiver bandwidth solutions, it has a very interesting behavior, but only around its optimal values. Moreover, it should be remembered that this is the only format that necessarily requires an external modulator (while all the other three modulation formats also can be implemented with directly modulated lasers).

– PAM-2 presents a strong filtering-dependent performance (see Fig. 6). For instance, by using two transceivers having the same $B_{3\,dB} = 30\%$ but very different steepness (i.e., $B_{20\,dB} = 60\%$ and 120%, which is not far from a real situation, as shown by the red points in Fig. 6), a very different penalty of >7 dB versus ~1 dB, respectively, can be obtained. Therefore, PAM-2 is a good alternative only if large bandwidth transceivers are used.
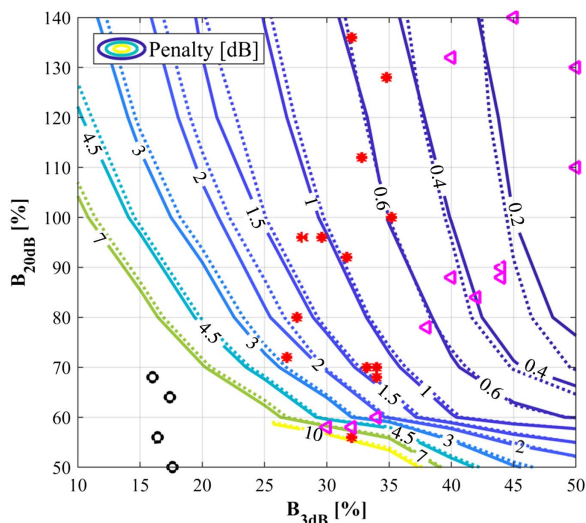
Fig. 6. PAM-2 power penalty with respect to the S obtained for PAM-2 in the best condition (BtB unlimited bandwidth case, $S_0 = -28.1$ dBm for 25 Gb/s and $S_0 = -25.7$ dBm for 50 Gb/s) as a function of the GFs $B_{3\,dB}$ and $B_{20\,dB}$ parameters. Red points: 25 Gb/s using 10G technology transceivers. Black circles: 50 Gb/s using 10G technology transceivers. Pink triangles: 50 Gb/s using 25G technology transceivers.
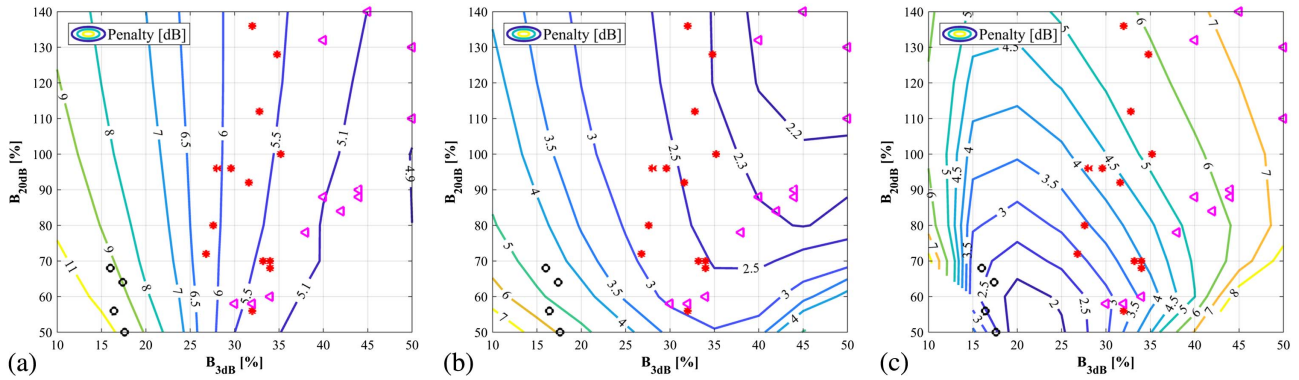
F7:1   Fig. 7.   (a) PAM-4, (b) EDB, and (c) ODB power penalty with respect to the S obtained for PAM-2 in the BtB unlimited bandwidth case, S_0
F7:2   ($S_0 = -28.1$ dBm for 25 Gb/s and $S_0 = -25.7$ dBm for 50 Gb/s) as a function of $B_{3\,dB}$ and $B_{20\,dB}$ of the GFs. Red points: 25 Gb/s using 10G
F7:3   technology. Black circles: 50 Gb/s using 10G technology. Pink triangles: 50 Gb/s using 25G technology.

585   – EDB shows a good tolerance against filtering, and a pen-
586   alty between 2 and 3 dB in all the cases reported in Table I.
587   Accordingly, EDB seems to be a very interesting alterna-
588   tive in terms of resilience against filtering variations (with
589   respect to both −3 dB bandwidth and steepness).

590   Let us now consider the option of transmitting 50 Gb/s
591   using 10G technology (50G/10G):

592   – PAM-2 is not feasible (see the black circles of Fig. 6).
593   – Neither PAM-4 or EDB seem to be feasible alternatives,
594   since a large power penalty is achieved in this situation
595   [see the black circles of Figs. 7(a) and 7(b)].
596   – The only modulation format that may be used is ODB
597   [see the black circles of Fig. 7(c)]. However, in the $B_{3\,dB} <$
598   15% range, the penalty of ODB rapidly increases even
599   with small −3 dB bandwidth decreases. Therefore, the
600   performance stability can be critical.

601   Finally, let us consider transmitting 50 Gb/s using 25G
602   technology (50G/25G):

603   – For PAM-2 and EDB, the same conclusions as in the case
604   of 25G/10G can be extrapolated. However, most 25G tech-
605   nology has more relaxed bandwidth limitations to trans-
606   mit 50 Gb/s (see pink triangles in Fig. 6). PAM-2 then
607   seems to be a good alternative to transmit 50G/25G.
608   EDB only outperforms it if transceivers with very strong
609   bandwidth limitations are employed.
610   – PAM-4 and ODB are not good candidates since a large
611   power penalty (>3 dB) arises in this situation.

V. DISPERSION ANALYSIS

613   In Section IV, the effect of the transceivers' filtering char-
614   acteristics on the performance of four IM/DD modulation
615   formats in a BtB scenario was analyzed. In this section,
616   the previous analysis is extended by also considering the
617   presence of chromatic dispersion in the link.

618   As a first approach, the $B_{3\,dB}$ and $B_{20\,dB}$ parameters are
619   fixed to some of the values discussed in the previous section

and the total dispersion of the link is varied to compute the   620
relative power penalty of the four modulation formats as a   621
function of this last parameter. For the 25 Gb/s transmis-   622
sion, two representative $\{B_{3\,dB}, B_{20\,dB}\}$ pairs were selected: 623
$P1 = \{32\%, 136\%\}$ and $P2 = \{32\%, 56\%\}$ (cases 5 and 3 of   624
Table I, respectively), to compare the power penalty versus   625
dispersion curves obtained when the −3 dB bandwidth of   626
the filters is the same, but the steepness is abruptly   627
changed. The results are displayed in Fig. 8(a). For the   628
50 Gb/s situation, the following $\{B_{3\,dB}, B_{20\,dB}\}$ pairs were   629
employed: $P3 = \{32\%, 132\%\}$ and $P4 = \{32\%, 58\%\}$ (case   630
5 of Table II). The corresponding results are shown in   631
Fig. 8(b).   632

From Fig. 8(a) ($R_b = 25$ Gb/s), we can observe that   633
PAM-4 is the most robust format against the effect of both   634
dispersion and filtering. EDB also exhibits good tolerance   635
against dispersion. We now introduce some practical con-   636
sideration focusing on the PON scenario, which requires   637
using SMF fibers up to $l = 20$ km in different wavelength   638
bands, which we have grouped as O-band (about 1300 nm,   639
where at the limit of the bandwidth specified by different   640
PON standards the accumulated dispersion can go   641
up to ∼100 ps/nm), C-band (1550 nm, accumulated   642
dispersion up to 360 ps/nm), and L-band (1580 nm, up   643
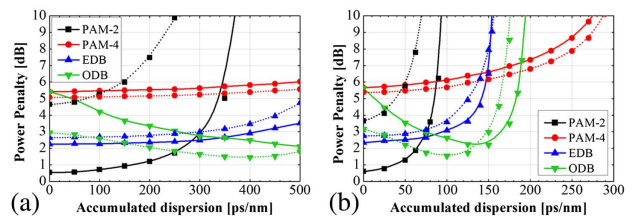to ∼460 ps/nm). Comparing the different modulation   644

(a)   (b)

Fig. 8.   Performance comparison among the four modulation   F8:1
formats in terms of the *relative power penalty* as a function   F8:2
of dispersion. (a) $R_b = 25$ Gb/s; solid: $B_{3\,dB} = 32\%$ and $B_{20\,dB} =$ F8:3
136%; dotted: $B_{3\,dB} = 32\%$ and $B_{20\,dB} = 56\%$; (b) $R_b = 50$ Gb/s;   F8:4
solid: $B_{3\,dB} = 32\%$ and $B_{20\,dB} = 132\%$; dotted: $B_{3\,dB} = 32$ GHz   F8:5
and $B_{20\,dB} = 58\%$. The power penalty is relative to PAM-2 S_0 F8:6
($S_0 = -28.1$ dBm for $R_b = 25$ Gb/s and $S_0 = -25.7$ dBm for   F8:7
$R_b = 50$ Gb/s).   F8:8

645 formats, EDB outperforms PAM-4 in O, C, and L optical
646 bands. Regarding PAM-2, as in BtB, in presence of
647 dispersion its performance is also highly affected by the
648 steepness of the out-of-band transceivers' response. Its
649 use in C- or L-band is not feasible for $l = 20$ km. In O-band,
650 its use seems to be strongly constrained to the use of tech-
651 nology with low steepness filtering characteristics. Under
652 these conditions, its performance is the best among all
653 modulation formats. ODB, on the other hand, is the only
654 format in which the performance improves as both the
655 dispersion and steepness of the filters increase (at least
656 in O, C, and L bands with $l = 20$ km). In O-band, ODB
657 is outperformed by EDB, while in the C- and L-bands it
658 seems to be the best alternative.

659 Regarding the 50 Gb/s transmission [see Fig. 8(b)] over
660 20 km of fiber, we observed that no modulation format can
661 be used to operate the system in the C-band or L-band.
662 PAM-2 does not work even in the O-band. The only feasible
663 modulation formats (in O-band, $l = 20$ km) are EDB, ODB,
664 and PAM-4, being the performance of PAM-4 surpassed by
665 that of both EDB and ODB in the whole O-band.

666 Although PAM-4 has been found to be the most resilient
667 format against dispersion and bandwidth limitations in all
668 the analyzed conditions, due to its higher intrinsic penalty
669 as compared to EDB in all the practical scenarios, we do not
670 consider it a feasible alternative for the implementation of
671 25 Gb/s or 50 Gb/s PON systems over 20 km of fiber.
672 Therefore, we do not analyze this modulation format in
673 the rest of this section. A similar consideration has been
674 performed with respect to PAM-2 operating in the C-band
675 with $R_b = 25$ Gb/s, and the O-band with $R_b = 50$ Gb/s.
676 Therefore, other than the 25 Gb/s O-band case in which
677 PAM-2 can still be considered a feasible format, the rest
678 of this section will be focused on the comparison between
679 EDB and ODB formats.

680 Some preliminary results allow us to forecast the fea-
681 sibility of PAM-2 and PAM-4 using pre-chirping in the
682 transmission of 50 Gb/s in the O-band and C-band
683 ($l = 20$ km), respectively, at least under relaxed bandwidth
684 limitations (1-pole BFs case). However, these alternatives
685 need to be further explored under more strict filtering

686 conditions, which is an analysis out of the scope of the
687 present contribution.

688 We now proceed with some further insight, focusing on
689 25 Gb/s transmission results. In Figs. 9 and 10 we show,
690 for the O-band and the C-band operation over 20-km of fi-
691 ber, respectively, the contour plots of the power penalty as a
692 function of $B_{3\,dB}$ and $B_{20\,dB}$, for different modulation for-
693 mats and for different accumulated dispersion (using the
694 previously indicated notation of the O- and the C-band
695 at 20 km). The power penalty is evaluated in all cases with
696 respect to S_0 of PAM-2 in BtB conditions ($S_0 = -28.1$ dBm
697 for $R_b = 25$ Gb/s).

698 Regarding O-band operation (Fig. 9), the three modula-
699 tion formats exhibit similar results to the BtB situation
700 (see Figs. 6 and 7), but have a small dispersion penalty
701 for PAM-2 and EDB. In contrast, ODB exhibits a perfor-
702 mance improvement thanks to dispersion, which is consis-
703 tent with the results presented in Fig. 8. The power penalty
704 of EDB varies between 2.2 and 3 dB when using state-of-
705 the-art transceivers with different -3 dB bandwidth and
706 out-of-band filtering steepness. In contrast, in the case of
707 PAM-2, this penalty can vary from around 0.6 to an exceed-
708 ingly large value around 10 dB. ODB is an intermediate
709 case (the penalty varies from 2.5 to 4.5 dB). Therefore,
710 we consider EDB as the best alternative for 25 Gb/s 20-
711 km O-band operation with respect to tolerance against
712 frequency response variations. However, PAM-2 can be a
713 good solution; its penalty can be as low as <1 dB, which
714 is a value not achievable by any other format, if *and*
715 *only if* technology with proper filtering characteristics
716 ($B_{3\,dB} \geq 30\%$ and $B_{20\,dB} \geq 70\%$) can be guaranteed.

717 When considering C-band operation, we can see from the
718 contour plots shown in Figs. 10(a) and 10(b), that the per-
719 formance of ODB is further improved by dispersion while
720 the opposite occurs for EDB. This situation tips the scales
721 in favor of ODB in terms of a lower range of power penalty
722 achievable using state-of-the-art devices (i.e., from 1 to
723 3 dB, in contrast to 2.5 to 3.5 dB achieved with
724 EDB). EDB remains the format with less performance var-
725 iations as a function of filtering. It is important to note that,
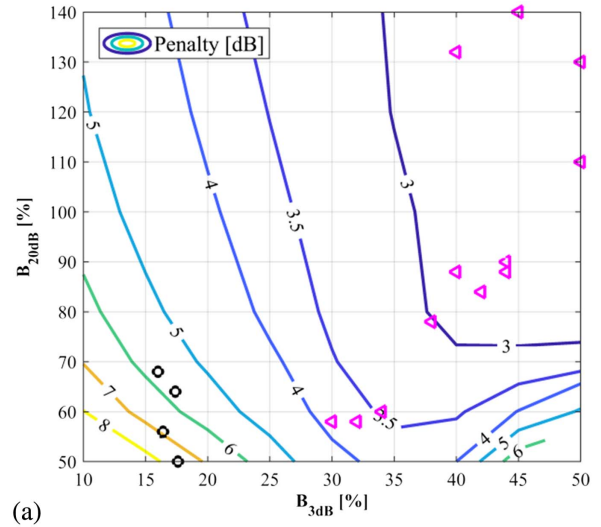726 by using ODB and small band-limited transceivers
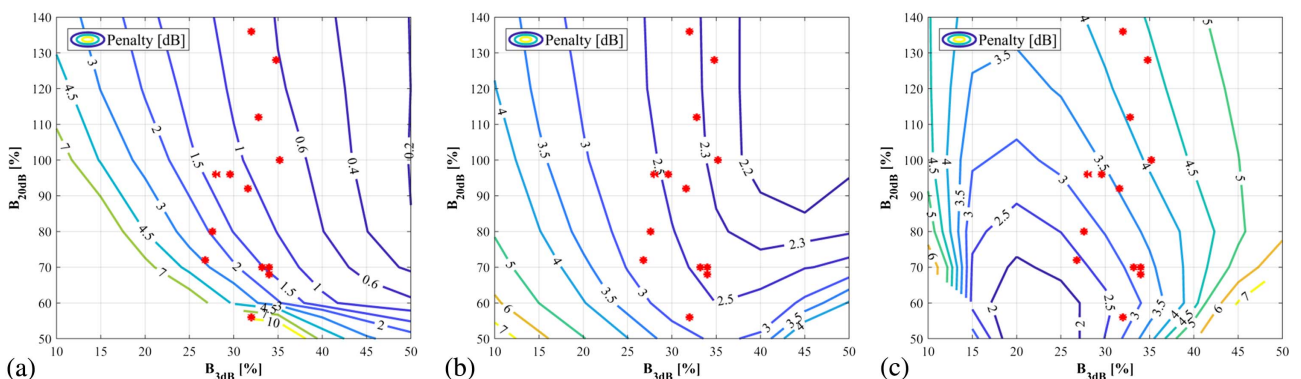
F9:1   Fig. 9.   (a) PAM-2, (b) EDB, and (c) ODB power penalty with respect to the S obtained for PAM-2 in the BtB unlimited bandwidth case, S_0
F9:2   ($S_0 = -28.1$ dBm) as a function of $B_{3\,dB}$ and $B_{20\,dB}$ of the GFs, for a 25 Gb/s 20 km O-band operation. Red points: 25 Gb/s using $10\overline{G}$
F9:3   technology.
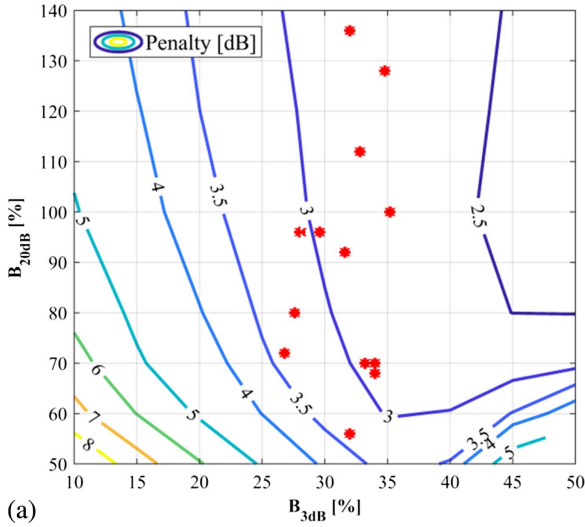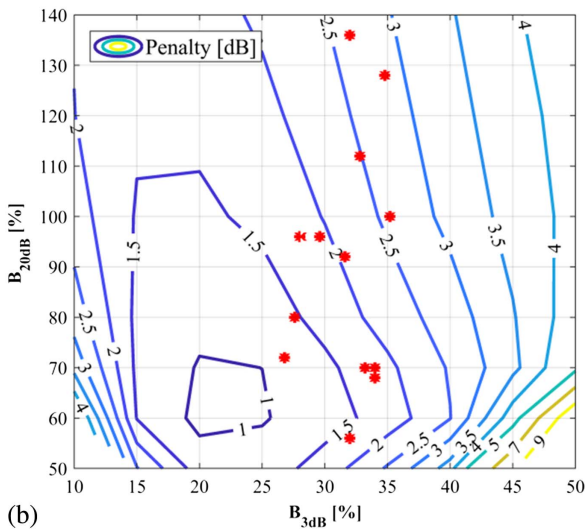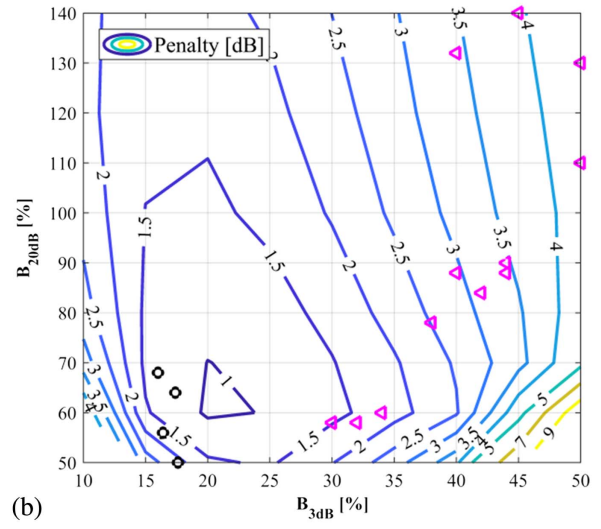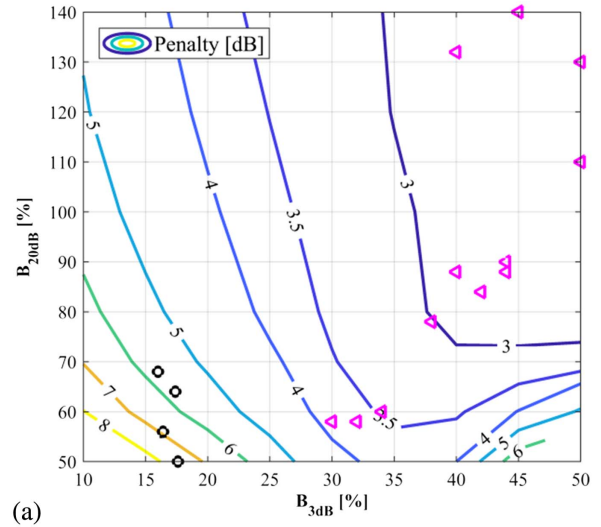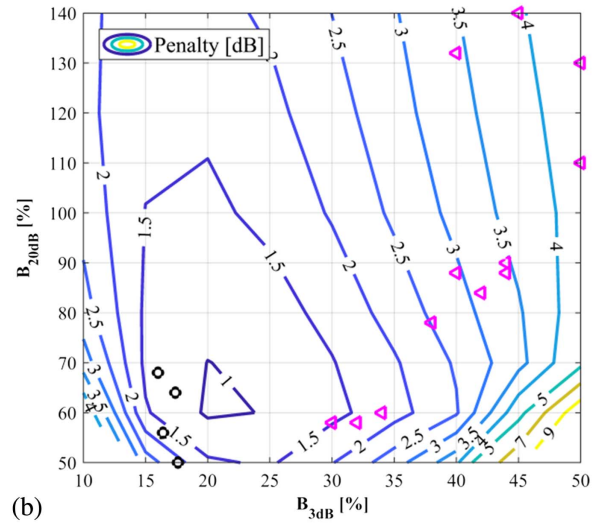
F10:1   Fig. 10.   (a) EDB and (b) ODB power penalty with respect to the S
F10:2   obtained for PAM-2 in the BtB unlimited bandwidth case, S_0
F10:3   ($S_0 = -28.1$ dBm) as a function of $B_{3\,dB}$ and $B_{20\,dB}$ of the GFs,
F10:4   for a 25 Gb/s20 km C-band operation. Red points: 25 Gb/s using
F10:5   10G technology.

Fig. 11.   (a) EDB and (b) ODB power penalty with respect to the S   F11:1
obtained for PAM-2 in the BtB unlimited bandwidth case, S_0 F11:2
($S_0 = -25.6$ dBm) as a function of $B_{3\,dB}$ and $B_{20\,dB}$ of the GFs,   F11:3
for a 50 Gb/s 20 km O-band operation. Black circles: 50 Gb/s us-   F11:4
ing 10G technology. Pink triangles: 50 Gb/s using 25G technology.   F11:5

727   (i.e., $B_{3\,dB} \geq 35\%$ and $B_{20\,dB} \geq 100\%$), it is always possible to
728   increase the performance of the system by intentionally
729   adding an electrical filter at the TX or RX, to enforce a
730   stronger band-limited condition [close to the optimum
731   point that can be seen in Fig. 10(b)] in which the achievable
732   penalty could be only 1 dB. This feature is not achievable
733   using any other modulation format. Another positive
734   (and unique) feature of ODB is that, as can be seen in Fig. 8,
735   the dispersion penalty decreases as the accumulated
736   dispersion increases (i.e., length), which can compensate,
737   to some degree, for the increase of fiber attenuation as
738   the fiber length augments. In favor of EDB is the fact that
739   it can be implemented with both direct modulation and
740   external modulation (using electro-absorption modulators
741   or a MZM) approaches, while ODB must use a MZM.

742   Let us finally comment on the 50 Gb/s transmission re-
743   sults. In Fig. 11, contour plots of the power penalty as a

function of $B_{3\,dB}$ and $B_{20\,dB}$ for 50 Gb/s 20-km O-band op-   744
eration using EDB [Fig. 11(a)] or ODB [Fig. 11(b)], are   745
shown. The power penalty is referred to the 50 Gb/s   746
PAM-2 $S_0 = -25.6$ dBm. The contour plots displayed in   747
Fig. 11 are very similar to those shown in Fig. 10 (for   748
25 Gb/s transmission in 20-km O-band). However, the re-   749
gions of operation of 50G/10G and 50G/25G state-of-the-art   750
devices (see the black circles and pink triangles of Fig. 11,   751
respectively) are different from those of 25G/10G (see the   752
red points of Fig. 10). Therefore, the conclusions between   753
these cases may differ. First, ODB appears to be the only   754
feasible format to transmit 50 Gb/s using 10G technology   755
in O-band. In the black circles of Fig. 11, only the cases 2, 3,   756
10, and 11 in Table I are plotted. The rest of the cases have   757
a $B_{20\,dB} < 50\%$, which corresponds to power penalties   758
higher than 2.5 dB [not shown in Fig. 11(b)]. Then, for   759

correct operation, the $B_{20\,dB}$ of the TX and RX should at least be higher than 50%.

Regarding the transmission of 50 Gb/s using 25G technology, the maximum penalty achievable with EDB [pink triangles in Fig. 11(a)] and ODB [pink triangles in Fig. 11(b)] is similar (around 4 dB). Again, EDB exhibits a more stable penalty, varying between 3 and 4 dB (mostly around 3 dB), while ODB penalty variation is wider, varying from 1.5 to 4 dB. In terms of tolerance against filtering, we should opt for EDB. However, as mentioned before, with the right technology characteristics or by enforcing the frequency response using an additional electrical filter, we could operate close to the optimal point of ODB and achieve a penalty as low as 1 dB.

VI. CONCLUSIONS

In this contribution, we have demonstrated the strong impact on system performance that the overall filter shaping electrical response of the transceivers has on the transmission of 25 and 50 Gb/s using currently available 10 and 25 Gb/s technology and adaptive equalization. Using numerical simulations, we compared the achievable performance of PAM-2, PAM-4, EDB, and ODB under different band-limited and dispersive conditions. We introduced the −20 dB bandwidth parameter to quantify the impact of the out-of-band steepness of the transceivers' response. We demonstrated that this parameter is as relevant as the −3 dB bandwidth when comparing the performance of different modulation formats.

We found that PAM-2 is the best performing format for the transmission of 25 Gb/s using 10G technology in the 20 km O-band, but only if transceivers with relatively small bandwidth limitations can be used. Otherwise, the best alternative is EDB because it is more resilient to filter shaping variations than PAM-2 and outperforms the rest of the formats in terms of penalty.

On the transmission of 25 Gb/s using 10G technology in 20-km C-band, EDB exhibits a slightly higher maximum power penalty than ODB (4 dB versus 3.5 dB). The minimum achievable power penalty of ODB is 1.5 dB lower than that of EDB. However, the performance of EDB as a function of the −3 dB and −20 dB bandwidth is more stable (power penalty variations are less than 1 dB) than in the case of ODB, which has power penalty variations up to 2 dB.

Regarding the 50 Gb/s case, no modulation format works under 20 km of C-band operation. PAM-2 is not even feasible in the O-band. ODB is the only format that can be used if using 10G technology (in the 20 km O-band), but only if some filtering conditions can be guaranteed. If 25G technology is used and the O-band is considered through 20 km of fiber, both EDB and ODB can work, exhibiting a maximum penalty of 4 dB. Again, the penalty of ODB is the minimum under some filtering conditions, but EDB performance is more robust against the filter shaping variations of the transceivers' frequency response.

In all cases, PAM-4 is the most robust format against both dispersion and filtering conditions. However, due to its inherent higher power penalty with respect to the rest of the formats, PAM-4 is always outperformed by any of them in most of the analyzed conditions.

The results presented in this contribution were obtained using identical filters to emulate the frequency response of both the TX and RX. For space limitations, we did not consider more general assumptions and degrees of freedom in our present analysis. Using filters with different characteristics at the TX and RX side, which could give rise to interesting results, is a topic we are currently researching.

REFERENCES

[1] IEEE P802.3ca 100G-EPON Task Force, "Physical layer specifications and management parameters for 25 Gb/s, 50 Gb/s, and 100 Gb/s passive optical networks," 2015 [Online]. Available: http://www.ieee802.org/3/ca/index.shtml.

[2] Full Service Access Network (FSAN), "Roadmap," 2016 [Online]. Available: https://www.fsan.org/roadmap/.

[3] ITU-T Study Group 15: Networks, "Technologies and infrastructures for transport, access and home," 2017 [Online]. Available: https://www.itu.int/en/ITU-T/studygroups/2017-2020/15/Pages/default.aspx.

[4] V. Houtsma, D. van Veen, and E. Harstead, "Recent progress on standardization of next-generation 25, 50, and 100G EPON," *J. Lightwave Technol.*, vol. 35, no. 6, pp. 1228–1234, 2017.

[5] D. Nesset, "PON roadmap [Invited]," *J. Opt. Commun. Netw.*, vol. 9, pp. A71–A76, 2017.

[6] D. van Veen, V. E. Houtsma, P. Winzer, and P. Vetter, "26-Gbps PON transmission over 40-km using duobinary detection with a low cost 7-GHz APD-based receiver," in *European Conf. Optical Communication (ECOC)*, Amsterdam, The Netherlands, 2012.

[7] Z. Li, L. Yi, X. Wang, and W. Hu, "28 Gb/s duobinary signal transmission over 40 km based on 10 GHz DML and PIN for 100 Gb/s PON," *Opt. Express*, vol. 23, pp. 20249–20256, 2015.

[8] D. van Veen, V. Houtsma, A. H. Gnauck, and P. Iannone, "Demonstration of 40-Gb/s TDM-PON over 42-km with 31 dB optical power budget using an APD-based receiver," *J. Lightwave Technol.*, vol. 33, no. 8, pp. 1675–1680, 2015.

[9] J. Wei, N. Eiselt, H. Griesser, K. Grobe, M. H. Eiselt, J. J. V. Olmos, I. T. Monroy, and J.-P. Elbers, "Demonstration of the first real-time end-to-end 40-Gb/s PAM-4 for next-generation access applications using 10-Gb/s transmitter," *J. Lightwave Technol.*, vol. 34, no. 7, pp. 1628–1635, 2016. **1**

[10] J. Man, S. Fu, H. Zhang, J. Gao, L. Zeng, and X. Liu, "Downstream transmission of pre-distorted 25-Gb/s faster-than-Nyquist PON with 10G-class optics achieving over 31 dB link budget without optical amplification," in *Optical Fiber Communication Conf. and Exhibition (OFC)*, Anaheim, California, 2016.

[11] D. van Veen and V. Houtsma, "Symmetrical 25-Gb/s TDM-PON with 31.5-dB optical power budget using only off-the-shelf 10-Gb/s optical components," *J. Lightwave Technol.*, vol. 34, no. 7, pp. 1636–1642, 2016.

[12] M. Tao, L. Zhou, S. Yao, D. Zou, S. Li, H. Lin, and X. Liu, "28-Gb/s/λ TDM-PON with narrow filter compensation and enhanced FEC supporting 31.5 dB link loss budget after 20-km downstream transmission in the C-band," in *Optical Fiber Communication Conf. and Exhibition (OFC)*, Anaheim, California, 2016.

[13] V. Houtsma and D. van Veen, "A study of options for high-speed TDM-PON beyond 10G," *J. Lightwave Technol.*, vol. 35, no. 4, pp. 1059–1066, 2017.

[14] C. Sun, S. H. Bae, and H. Kim, "Transmission of 28-Gb/s duobinary and PAM-4 signals using DML for optical access network," *IEEE Photon. Technol. Lett.*, vol. 29, no. 1, pp. 130–133, 2017.

[15] D. van Veen and V. Houtsma, "Proposals for cost-effectively upgrading passive optical networks to a 25G line rate," *J. Lightwave Technol.*, vol. 35, no. 6, pp. 1180–1187, 2017.

[16] T. Minghui, L. Zhou, H. Zeng, S. Li, and X. Liu, "50-Gb/s/λ TDM-PON based on 10G DML and 10G APD supporting PR10 link loss budget after 20-km downstream transmission in the O-band," in *Optical Fiber Communication Conf. and Exhibition (OFC)*, Los Angeles, California, 2017.

[17] S. Yin, V. Houtsma, D. van Veen, and P. Vetter, "Optical amplified 40-Gbps symmetrical TDM-PON using 10-Gbps optics and DSP," *J. Lightwave Technol.*, vol. 35, no. 4, pp. 1067–1074, 2017.

[18] D. Liu and M. Tao, "50G single wavelength PON analysis and comparison," in *IEEE 802.3 NG-EPON Study Group Meeting*, Orlando, Florida, Nov. 2017 [Online]. Available: http://www.ieee802.org/3/ca/public/meeting_archive/2017/11/liu_3ca_2a_1117.pdf.

[19] A. Stark and T. Detwiler, "Equalization strategies for 25G PON," in *Optical Fiber Communication Conf. and Exhibition (OFC)*, Los Angeles, California, 2017.

[20] R. Bonk, W. Poehlmann, D. van Veen, J. Galaro, R. Farah, H. Schmuck, and T. Pfeiffer, "The underestimated challenges of burst-mode WDM transmission in TWDM-PON," *Opt. Fiber Technol.*, vol. 26, pp. 59–70, 2015.

[21] J. Rue, M. Itzler, N. Agrawal, S. Bay, and W. Sherry, "High performance 10 Gb/s PIN and APD optical receivers," in *Electronic Components and Technology Conf.*, San Diego, California, 1999, pp. 207–215.

[22] N. Duan, T.-Y. Liow, A. E.-J. Lim, L. Ding, and G. Q. Lo, "310 GHz gain-bandwidth product Ge/Si avalanche photodetector for 1550 nm light detection," *Opt. Express*, vol. 20, pp. 11031–11036, 2012.

[23] G. P. Agrawal, *Fiber-Optic Communication Systems*, 3rd ed. Wiley, 2002.

[24] J. G. Proakis, *Digital Communications*, 4th ed., McGraw-Hill, 2000.

[25] J. G. Proakis and D. G. Manolakis, *Digital Signal Processing. Principles, Algorithms, and Applications*, 4th ed. Prentice Hall, 1996.

[26] S. Bottacchi, *Theory and Design of Terabit Optical Fiber Transmission Systems.*, Cambridge University, 2014.

[27] G. L. Li, T. G. B. Mason, and P. K. L. Yu, "Analysis of segmented traveling-wave optical modulators," *J. Lightwave Technol.*, vol. 22, no. 7, pp. 1789–1796, 2004.

[28] Spectrolab, "043643: 10 Gb/s InGaAs/InAlAs avalanche photodetector (APD) die," 2017 [Online]: Available: http://www.spectrolab.com/sensors/pdfs/products/SR%20APD%2010G%20Die_RevA%20052512.pdf.

[29] Y. Kang, M. Zadka, S. Litski, G. Sarid, M. Morse, M. J. Paniccia, Y.-H. Kuo, J. Bowers, A. Beling, H.-D. Liu, D. C. McIntosh, J. Campbell, and A. Pauchard, "Epitaxially-grown Ge/Si avalanche photodiodes for 1.3 μm light detection," *Opt. Express*, vol. 16, pp. 9365–9371, 2008.

[30] F. Effenberger, "NRZ-NFC for 28G-PON," in *IEEE 802.3 NG-EPON Study Group Meeting*, Dallas, Texas, Nov. 2015 [Online]. Available: http://www.ieee802.org/3/NGEPONSG/public/2015_11/ngepon_1511_effenberger_3.pdf

[31] M. Chagnon, M. Osman, M. Poulin, C. Latrasse, J.-F. Gagné, Y. Painchaud, C. Paquet, S. Lessard, and D. Plant, "Experimental study of 112 Gb/s short reach transmission employing PAM formats and SiP intensity modulator at 1.3 μm," *Opt. Express*, vol. 22, pp. 21018–21036, 2014.

[32] A. Samani, M. Chagnon, D. Patel, V. Veerasubramanian, S. ❷ Ghosh, M. Osman, Q. Zhong, and D. V. Plant, "A low-voltage 35-GHz silicon photonic modulator-enabled 112-Gb/s transmission system," *IEEE Photon. J.*, vol. 7, no. 3, pp. 1–13, 2015. ❸

[33] V. Houtsma, D. van Veen, A. Gnauck, and P. Iannone, "APD-based duobinary direct detection receivers for 40 Gbps TDM-PON," in *Optical Fiber Communications Conf. and Exhibition (OFC)*, Los Angeles, California, 2015.

[34] Z. Huang, C. Li, D. Liang, K. Yu, C. Santori, M. Fiorentino, W. Sorin, S. Palermo, and R. G. Beausoleil, "25 Gbps low-voltage waveguide Si-Ge avalanche photodiode," *Optica*, vol. 3, pp. 793–798, 2016.

[35] H. H. Lee, K.-H. Doo, S.-G. Mun, K. Kim, J. H. Lee, S.-K. Kang, H. Park, N. Park, H. Park, and H. S. Chung, "Real-time demonstration of QoS guaranteed 25-Gb/s PON prototype with Ethernet-PON MAC/PHY and cost-effective APD receivers for 100-Gb/s access networks," *Opt. Express*, vol. 24, pp. 13984–13991, 2016.

[36] M. Nada, M. Nakamura, and H. Matsuzaki, "25-Gbit/s burst-mode optical receiver using high-speed avalanche photodiode for 100-Gbit/s optical packet switching," *Opt. Express*, vol. 22, pp. 443–449, 2014.

Pablo Torres-Ferrera received B.E., M.E.E., and Ph.D. degrees (with honors) in Telecommunications in 2010, 2012, and 2017, respectively, from the National Autonomous University of Mexico (UNAM), Mexico City. He worked from 2012 to 2013 at Huawei Technologies Mexico in the implementation of OTN rings. As part of his Ph.D. investigation work, he carried out research internships at Athens Information Technology (AIT), Greece, in 2014 and at Politecnico di Torino, Italy, in 2016. He is currently a postdoctoral researcher at Politecnico di Torino, working in the field of high-speed optical access networks.

Valter Ferrero (M'97) received the Laurea degree (summa cum laude) in Electronics Engineering in 1994 from Politecnico di Torino, Italy. In 1994, he collaborated with Politecnico di Torino, working on coherent optical systems. From 1995 to 1996, he was with GEC Marconi, Genova, Italy. In 1997, he was in charge of the Optical Laboratory, Department of Electrical Engineering, Politecnico di Torino, and became Assistant Professor in 2001. He is currently with the Optical Communications Group, Politecnico di Torino. His current research interests include optical coherent communications, free-space optical communications, and next-generation passive optical networks.

Maurizio Valvo received a M.Sc. degree in Electronics Engineering cum laude at the University of Naples (Italy) in

1991. In the same year, he joined CSELT, the Telecommunications Research Centre and Laboratories, which is now TIM Lab–Turin and where he is currently active. He has focused since the beginning of his career on broadband access networks and, in particular, on PON systems, which he has also contributed to specify, develop, and test during the 1990s in the framework of several European-funded projects. He has led research projects with the objective to specify and test, both in the laboratory and in the field, innovative access network technologies based on PON, xDSL, HFC, Wimax, and free space optics. He currently leads the laboratory for fixed access network innovation and a research project for the innovation of the Telecom Italia optical access network. He holds four patents and is the co-author of three books and several papers.

Roberto Gaudino, Ph.D., is currently an associate professor at Politecnico di Torino, Italy. His main research interests are in long-haul DWDM systems, fiber nonlinearity, modeling of optical communication systems, and in the experimental implementation of optical networks, with a specific focus on access networks. In particular, in the last five years, he focused his activity on short-reach optical links using plastic optical fibers (POF) and on next-generation passive optical access networks (NG-PON2). Currently, he is working on ultra-high-capacity systems for medium-reach links. Previously, he worked extensively on fiber modeling, optical modulation formats, coherent optical detection, and on the experimental demonstration of packet-switched optical networks. He is the author or co-author of more than 200 papers in the field of optical communications. From 2009 to 2016, he was the coordinator of three projects in the area of optical access (EU FP6-IST STREP "POF-ALL" and "POF-PLUS" and EU FP7-ICT STREP project "FABULOUS"). He is now the coordinator of the PhotoNext center at POLITO.

Queries

1. AU: For Ref. [9], I have replaced the et al. with the names of the other authors based on this reference: https://www.osapublishing.org/jlt/abstract.cfm?uri=jlt-34-7-1628Please confirm that the change is correct.

2. AU: Please provide all the author names in place of "et al." in 'Ref. [32]' as per journal style requirement.

3. AU: For Ref. [32], I have added the author names, based on this reference:http://ieeexplore.ieee.org/document/7096918/authors?ctx=authorsPlease confirm that this change is correct.